Cellular Physiology and Biochemistry

Cell Physiol Biochem 2018;47:1497-1508

DOI: 10.1159/000490866

Published online: June 25, 2018

Accepted: April 13, 2018

Original Paper

Effects of the TLR4/Myd88/NF-κB Signaling Pathway on NLRP3 Inflammasome in Coronary Microembolization-Induced Myocardial Injury

Qiang Su[a,c] Lang Li[a] Yuhan Sun[a] Huafeng Yang[a] Ziliang Ye[a] Jinmin Zhao[b,c]

[a]Department of Cardiology, The First Affiliated Hospital of Guangxi Medical University, Nanning, [b]Department of Trauma Orthopedic and Hand Surgery, The First Affiliated Hospital of Guangxi Medical University, Nanning, [c]Guangxi Key Laboratory of Regenerative Medicine, Guangxi Medical University, Guangxi, China

Key Words
TLR4 • Coronary microembolization (CME) • Myocardial injury • Inflammation • NLRP3

Abstract
Background/Aims: Coronary microembolization (CME) is a common complication of acute coronary syndrome (ACS) and percutaneous coronary intervention (PCI); Myocardial inflammation, caused by CME, is the main cause of cardiac injury. TLR4/MyD88/NF-κB signaling plays an important role in the development of myocardial inflammation, but its effects on CME remain unclear. To assess the cardiac protective effects of TAK-242 (TLR4 specific inhibitor) on CME-induced myocardial injury, and explore the underlying mechanism. ***Methods:*** Cardiac function, serum c-troponin I level, microinfarct were examined by cardiac ultrasound, myocardial enzyme assessment, HBFP staining. The levels of TLR4/MyD88/NF-κB signaling and NLRP3 inflammasome pathway were detected by ELISA, qRT-PCR and western blot. ***Results:*** The results showed inflammatory responses in the myocardium after CME, with increased expression levels of pro-inflammatory factors TNF-α, IL-1β and IL-18. Meanwhile, TLR4/MyD88/NF-κB signaling and the NLRP3 inflammasome were involved in the inflammatory process. TAK-242 administration before CME effectively inhibited the inflammatory response in the rat myocardium after CME and reduced myocardial injury, mainly by inhibiting TLR4/MyD88/NF-κB signaling and reducing NLRP3 inflammasome activation. In addition, *in vitro* assays with neonatal rat cardiomyocytes further confirmed that TLR4/MyD88/NF-κB signaling was significantly activated in the inflammatory response of LPS-induced cardiomyocytes, via activation of the NLRP3 inflammasome. Inhibition of TLR4/MyD88/NF-κB signaling resulted in increased survival of cardiomyocytes mainly by reducing the release of inflammatory

Jinmin Zhao and Lang Li

Department of Trauma Orthopedic and Hand Surgery, The First Affiliated Hospital of Guangxi Medical University, Nanning, 530021 (China)
E-Mail drzhaojinmin@163.com / drlangli@yeah.net

cytokines and decreasing NLRP3 inflammasome activation. ***Conclusions:*** TLR4/MyD88/NF-κB signaling participates in the inflammatory response of the myocardium after CME, activating the NLRP3 inflammasome, promoting the inflammatory cascade, and aggravating myocardial injury. Blocking TLR4/MyD88/NF-κB signaling may help reduce myocardial injury and improve cardiac function after CME.

Introduction

Coronary microembolization (CME) is a complex complication of distal microvascular embolism caused by the shedding of atheromatous plaque debris in acute coronary syndrome (ACS) and percutaneous coronary intervention (PCI), and constitutes an independent and strong predictor of long-term prognosis and major adverse cardiac events [1, 2]. Studies showed that large amounts of inflammatory cells infiltrate the myocardial microinfarction, with a massive release of inflammatory factors, leading to local inflammation in the myocardium, which is the main reason for myocardial injury and progressive cardiac dysfunction after CME [3]. Further reports revealed that extensive activation of NF-κB and the release of inflammatory mediators, such as TNF-α and IL-1β, play important roles in CME-related progressive heart failure as well as advanced heart failure; after NF-κB inhibition by its specific inhibitor PDTC, CME-induced local inflammation in the myocardium is significantly weakened, with markedly improved cardiac function [4, 5]. Therefore, activation of NF-κB signaling and the massive release of various inflammatory mediators play important roles in CME-induced myocardial injury. However, the underlying molecular mechanisms remain unclear.

Toll-like receptor (TLRs) belong to pattern recognition receptors (PRRs), which constitute an important part of the innate immune system [6]. Toll-like receptor 4 (TLR4), the first described member of the TLR family, mediates the inflammatory response in the myocardium; in addition, its mediated inflammatory signaling pathway plays a key role in myocarditis, myocardial infarction, and ischemia-reperfusion injury [7-9]. Multiple studies have demonstrated that TLR4/MyD88/NF-κB signaling controls the production of pro-inflammatory factors and induces the inflammatory response in the myocardial tissues, which is the main cause of myocardial tissue injury [10, 11]. In addition, TLR4/MyD88/NF-κB signaling also promotes the inflammatory cascade by activating nod-like receptor protein 3 (NLRP3), aggravating myocardial injury [12]. Our previous studies found that TLR4 expression levels in the rat myocardial tissues increase significantly after CME, while treatment with its specific inhibitor TAK-242 results in markedly reduced TLR4 expression in the myocardium, with significantly improved cardiac function and reduced myocardial injury [13]; however, the exact underlying mechanism remains unclear. Therefore, the effects of TAK-242 on lipopolysaccharide (LPS)-treated myocardial cells and inflammatory responses in the myocardial tissues of rats with CME were evaluated in this study, assessing the role of the TLR4/MyD88/NF-κB signaling pathway. Our findings provide novel insights into the molecular mechanisms of CME-induced inflammatory response in the myocardium as well as cardiac dysfunction.

Materials and Methods

Animal

All experimental protocols were approved by the Institutional Animal Care and Use Committee at Guangxi Medical University, and the procedures were performed in compliance with the National Institutes of Health Guidelines on the Use of Laboratory Animals. Forty male Sprague-Dawley (SD) rats (250-300g) were obtained from the medical experimental animal center of Guangxi Medical University. The animals were housed under a 12h/12h light/dark cycle at 25°C, with free access to standard rat food and tap water.

Establishment of the CME model and grouping

According to Li et al [14]., intraperitoneal injection of pentobarbital hydrochloride (30~40 mg/kg) was performed for anaesthesia, after which tracheotomy and intubation were carried out; a small animal ventilator was used for assisted respiration. The chest was opened between the third and fourth ribs of the left margin of the sternum; then, the ascending aorta was separated and clamped for 10 seconds with a vascular clamp, and 3000 microemboli (diameter, 42μm, Biosphere Medical Inc. Rockland, USA) were quickly injected from the apical part of the left ventricle with a micro injector (microemboli were resuspended in 0.1 m1 normal saline). The chest was closed after a steady heartbeat, with the trachea cannula removed after stable breathing. After the operation, 800, 000 units of penicillin were administered intraperitoneally. The rats were fed with standard diet. The same operation was performed by injecting normal saline (0.1 ml) to the sham group. A total of 40 SD rats were randomly divided into groups, including the sham, CME, CME plus TAK-242 (CME+TAK-242), and sham plus TAK-242 (sham+TAK-242) groups (n=10 per group). In the CME+TAK-242 group, tail vein injection of TAK-242 (2 mg/kg, MedChem Express, Princeton, USA) was performed 30 minutes before CME modelling; the sham+TAK-242 group was administered TAK-242 (2 mg/kg) by tail vein 30 minutes sham treatment.

Cardiac function assessment

Preliminary experiments showed that cardiac function 6 hours after CME was lowest [15]. Therefore, the 6-hour time point was selected as the observation point. A Hewlett Packard Sonos 7500 ultrasound instrument (Philips Technologies, USA) was used to assess left ventricular ejection fraction (LVEF), left ventricular end diastolic diameter (LVEDd), left ventricular fractional shortening (LVFS) and cardiac output (CO) in the animals, with a probe frequency of 12 MHz. Values were averaged from three cardiac cycles. All echocardiographic examinations were performed by a specialist with extensive experience in echocardiography.

Measurement of serum c-troponin I levels

Blood (1.0 ml) was obtained from the femoral vein in each rat at 6h after sham operation or CME prior to sacrifice. Then, serum c-troponin I levels were assessed by the electro-chemistry method according to the manufacturer's instruction (Roche, Inc, Switzerland).

Tissue sampling and treatment

After cardiac function assessment, 10% potassium chloride injection (2 mL) was injected by tail vein in rats. Upon cardiac arrest in the ventricular diastolic phase, the heart was immediately extracted, and the atrial appendage and atrium were removed. Parallel to the atrioventricular sulcus, in the middle point of the long axis of the left ventricle, the ventricle was divided into the apex and bottom; the apex was snap frozen in liquid nitrogen and stored at -80°C for fluorescence quantitative PCR and Western blot. Meanwhile, the bottom of the heart was fixed with 4% polyoxymethylene for 12 hours, paraffin embedded and continuously sliced (4μm thickness). Hematoxylin-eosin (H&E) and hematoxylin basic fuchsine picric acid (HBFP) staining methods were performed to assess the micro-infarcted area of the myocardium.

Measurement of micro-infarcted area of the myocardium

HBFP staining is an important staining method for the diagnosis of early myocardial ischemia; in the ischemic myocardium, red blood cells appear red, the normal myocardial cytoplasm is stained yellow, and the nucleus appears blue. The DMR+Q550 Pathological image analyser (Leica, Wetzlar, Germany) was used for the examination of 5 randomly selected high power fields per slice (magnification, ×100). The Leica Qwin analysis software was used to measure the infracted area, which was expressed as the percentage of total analyzed slice [16].

Assessment of serum and cell supernatant levels of inflammatory cytokines by enzyme-linked immunosorbent assay (ELISA)

The levels of IL-1β, IL-18, and TNF-α in serum samples and cell supernatants were examined with specific ELISA kits (R&D Systems, Minneapolis, MN, USA) according to the manufacturer's instructions.

Cell culture and treatment

The hearts from 1-2-day old SD rats (Medical Experimental Animal Center of Guangxi Medical University, China) were dissected and placed in cold PBS. The cardiomyocytes were isolated by treatment with a combination of collagenase type II (Sigma, USA) and trypsin. Cardiomyocytes were pre-plated twice for 1h to minimize contamination by non-myocytes, and cultured in Dulbecco's modified Eagle's medium (DMEM) containing 20% FBS (Gibco, Australia) at 37°C in a humidified atmosphere containing 5% CO2. The medium was changed the next day to 10% FBS DMEM. Three days after seeding, the cardiomyocytes were incubated with TAK-242 (1μM) according to the manufacturer's instructions in the presence or absence of 10μg/ml LPS for 12h [17].

Cell viability assay

Cardiomyocytes were plated at a density of 2.0×10^5 cells/well in 96-well plates. After treatment, cell viability was assessed with Cell Counting Kit-8 (Dojindo Laboratory, Kumamoto, Japan) following the manufacturer's protocol. The relative amounts of viable cells were determined in duplicate, based on untreated cells.

RNA extraction and quantitative real-time PCR (qRT-PCR)

Total RNA was extracted from cardiac tissues and cardiomyocytes using the TRIzol reagent (Gibco, USA) according to the protocols supplied by the manufacturers. The concentration of RNA was quantified by a NanoDrop (Thermo Fisher Scientific Inc., USA) and then subjected to reverse transcription using a cDNA reverse transcription kit (TaKaRa, Japan) according to the manufacturer's instructions. Then, the obtained cDNA was subjected to RT-qPCR for TLR4 mRNA using a SYBR Green I PCR kit (TaKaRa, Japan). The conditions for all RT-qPCR reactions were performed on the ABI PRISM 7500 system (Applied BioSystems, USA). Glyceraldehyde-3-phosphate dehydrogenase (GAPDH) was used as an internal control. The sequences of the primers were designed as follows: TLR4 forward: 5′-AAGTTATTGTGGTGGTGTCTAG-3′ and reverse: 5′-GAGGTAGGTGTTTCTGCTAAG-3′. GAPDH forward: 5′-TGCACCACCAACTGCTTAG-3′ and reverse: 5′-GATGCAGGGATGATGTTC-3′. The relative quantification of TLR4 mRNA expression was calculated using the $2^{-\Delta\Delta Ct}$ method and was normalized to GAPDH.

Western blot

Total protein samples obtained from cardiac tissues and cardiomyocytes were separated by 10%-15% SDS-PAGE and electro-transferred onto PVDF membranes (Millipore, Atlanta, GA, US). The membranes were blocked with 5% bovine serum albumin or non-fat milk for 1.5h at room temperature and incubated at 4°C overnight with primary antibodies raised against TLR4, MyD88, NF-κB p65, NLRP3, ASC, Caspase-1 or GAPDH. Primary antibodies specific to TLR4, NLRP3, and ASC were supplied by Abcam Biotech (Cambridge, UK). Primary antibodies targeting MyD88, NF-κB p65, and Caspase-1 were obtained from Cell Signaling Technology (Beverly, MA, USA). After washing with TBS containing 0.1% Tween 20 (TBST) for 5 times, the membranes were incubated with secondary antibodies conjugated with horseradish peroxidase in TBST for 2h at room temperature. Immunoreactive bands were detected with an enhanced chemiluminescence detection system (Pierce, Rockford, IL, USA), and protein amounts were quantified with the Image Lab software (Bio-Rad).

Statistical Analysis

Data are mean±standard error of mean (SEM). Groups were compared by one way ANOVA, with $P<0.05$ considered statistically significant. Statistical analyses were performed with the GraphPad Prism software version 5.0 (GraphPad Software, Inc., San Diego, CA).

Results

Changes of cardiac function

LVEF, FS, CO, and LVEDd detected by cardiac ultrasound were used to evaluate cardiac function in rats. Data obtained at 6 hours post-operation are shown in Table 1. Compared with the sham group, the CME group showed significantly decreased cardiac function, as

reflected by myocardial contractile dysfunction and left ventricular dilatation, i.e. decreased LVEF, FS, and CO (P<0.05), and increased LVEDd (P<0.05). In addition, cardiac injury was improved in the CME+TAK-242 group compared with the CME group, as reflected by elevated LVEF, FS, and CO (P<0.05) and reduced LVEDd (P<0.05). However, there was no significant difference in cardiac function between the sham+TAK-242 nd sham groups (P>0.05).

Levels of the myocardial injury marker cTnI in various groups

Compared with the sham group, the CME group showed markedly increased serum cTnI levels (0.59±0.08 ng/ml vs. 0.017±0.008 ng/ml, P<0.05). Serum cTnI levels in the CME+TAK-242 group were decreased significantly compared with those of the CME group (0.22±0.05 ng/ml vs. 0.59±0.08 ng/ml, P<0.05). However, there was no significant difference in serum cTnI amounts between the sham and sham+TAK-242 groups (0.019±0.007 ng/ml vs. 0.017±0.008 ng/ml, P>0.05) (Fig. 1).

Pathological findings

H&E and HBFP staining data are summarized in Fig. 2. In the sham and sham+TAK-242 groups, subendocardial ischemia can be observed occasionally, and overt infarcted lesions were absent. In the CME and CME+TAK-242 groups, micro-infarcted lesions were

Table 1. Changes in cardiac function ($\bar{x}$ ±s). LVEF, left ventricle ejection fraction; CO, cardiac output; LVEDd, left ventricular end-diastolic diameter; LVFS, left ventricle fractional shortening; CME, coronary microembolization. *P<0.05 vs. sham group; #P<0.05 vs. CME group

Group	n	LVEF (%)	LVFS (%)	CO (L/min)	LVEDd (mm)
sham	10	78.41±3.29	41.23±4.37	0.188±0.022	5.73±0.36
CME	10	58.76±2.81*	21.07±2.65*	0.103±0.008*	7.83±0.55*
CME+TAK-242	10	70.53±3.56#	35.49±4.15#	0.165±0.017#	6.52±0.46#
sham+TAK-242	10	77.34±3.28	40.36±4.19	0.179±0.024	5.89±0.41

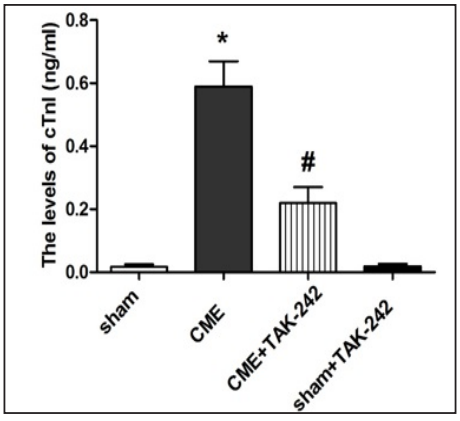

Fig. 1. Levels of cTnI in various rat groups. CME, coronary microembolization. *P<0.05 vs. sham group; #P<0.05 vs. CME group.

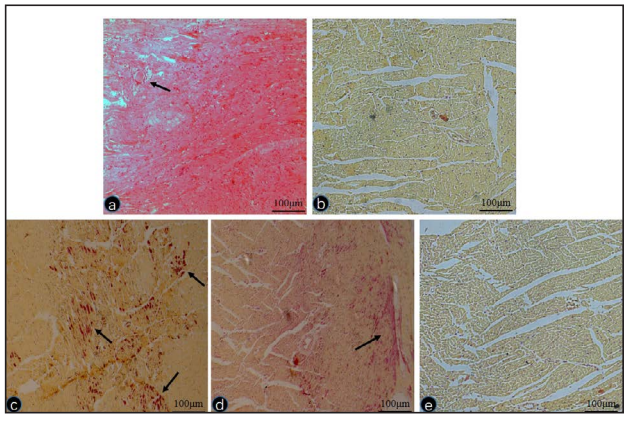

Fig. 2. Histopathological features as assessed by the H&E and HBFP staining methods. a: H&E staining of local micro-infracted lesions in the myocardium in the CME group; arrow indicates microspheres (×400); b-e: HBFP staining of samples from the sham, CME, CME+TAK-242, and sham+TAK-242 groups, respectively; ischemic myocardium appeared red. Arrow indicates a micro-infracted lesion (×200). *P<0.05 vs. sham group; #P<0.05 vs. CME group.

observed; most of them were wedge-shaped, focally distributed, and located under the endocardium and in left ventricle. H&E staining showed that myocardial nuclei in micro-infarcted lesions were dissolved or disappeared, and the cytoplasm appeared red; edema, degeneration, inflammatory cell infiltration, and erythrocyte exudation occurred in the myocardial periphery, with microemboli in the arterioles. The infarct sizes in the CME and CME+TAK-242 groups were 11.57±3.32% and 7.14±2.61%, respectively, indicating a significant decrease in the CME+TAK-242 group compared with the CME group (P<0.05).

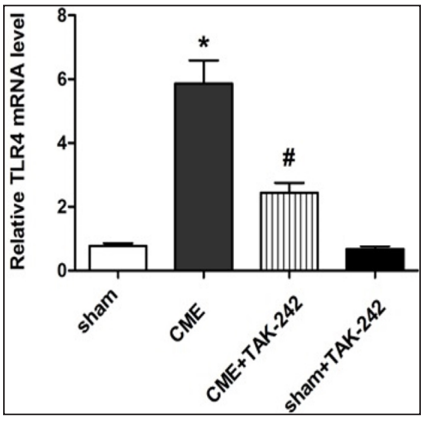

Fig. 3. TLR4 mRNA levels in the rat myocardium as detected by fluorescence quantitative PCR. CME, coronary microembolization. *P<0.05 vs. sham group; #P<0.05 vs. CME group.

TLR4/MyD88/NF-κB signaling is involved in myocardial inflammation after CME and NLRP3 inflammasome activation

As shown by qRT-PCR (Fig. 3), TLR4 mRNA levels in the CME group were increased significantly compared with those of the sham group (P<0.05). Meanwhile, TLR4 mRNA amounts in the CME+TAK-242 group were lower than those of the CME group. TLR4 mRNA levels were somewhat lower in the sham+TAK-242 group compared with the sham group, but with no significant difference (P>0.05). Western blot (Fig. 4) showed that TLR4, MyD88, and NF-κB p65 protein levels were markedly increased after modelling compared with the sham group; besides, the NLRP3 inflammasome was activated significantly, as reflected by significantly increased NLRP3, ASC, and caspase-1 levels (P<0.05). Compared with the CME group, protein expression levels of TLR4, MyD88, and NF-κB p65 in the CME+TAK-242 group were decreased significantly, and the NLRP3 inflammasome inhibited, as reflected by markedly reduced NLRP3, ASC, and Caspase-1 amounts (P<0.05). However, there were no significant differences in the expression levels of TLR4, MyD88, NF-κB p65, NLRP3, ASC, and caspase-1 between the sham+TAK-242 and sham groups (P>0.05).

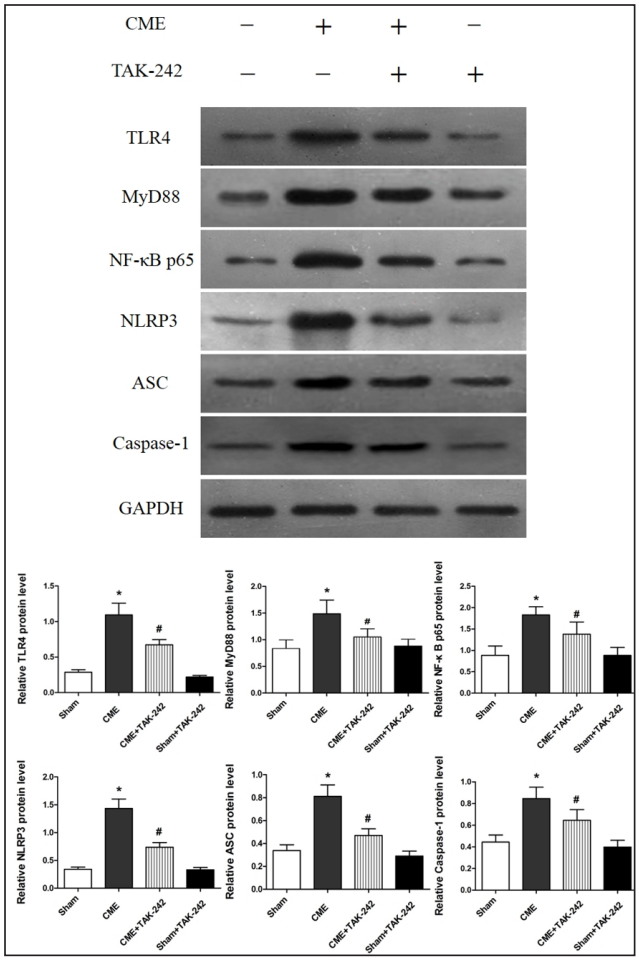

Fig. 4. TAK-242 inhibits CME-induced TLR4 upregulation and NLRP3 inflammasome activation. CME, coronary microembolization; NLRP3, Nod-like receptor protein 3. *P<0.05 vs. sham group; #P<0.05 vs. CME group.

Cytokine levels were assessed by ELISA (Fig. 5). Compared with the sham group, serum expression

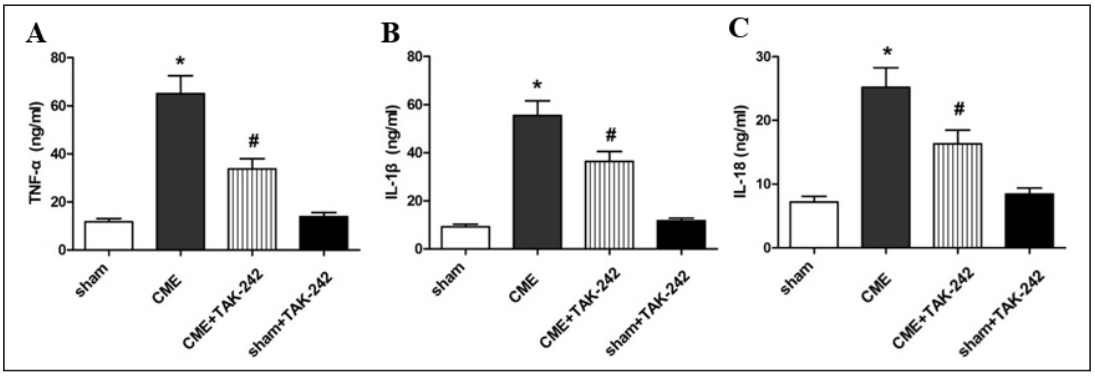

Fig. 5. Effects of TAK-242 on serum levels of TNF-α. (A), IL-1β (B), and IL-18 (C)CME, coronary microembolization. *P<0.05 vs. sham group; #P<0.05 vs. CME group.

levels of TNF-α, IL-1β, and IL-18 in the CME group were increased significantly (P<0.05); meanwhile, serum TNF-α, IL-1β, and IL-18 levels in the CME+TAK-242 group were lower than those pf the CME group (P<0.05). There were no significant differences in serum expression levels of TNF-α, IL-1β, and IL-18 between the sham+TAK-242 and sham groups (P>0.05).

The above results suggested that the TLR4/MyD88/NF-κB pathway participated in the process of myocarditis after CME and promoted NLRP3 inflammasome activation.

Cell viability after LPS challenge

As shown in Fig. 6, the survival rate of cardiomyocyte decreased significantly after 12 hours of LPS stimulation (P<0.05) after TAK-242 pre-treatment, the survival rate significantly increased (P<0.05). However, cardiomyocytes pre-treated with TAK-242 alone showed no significant change in survival rate in comparison with control untreated cardiomyocytes (P<0.05).

TLR4/MyD88/NF-κB signaling is involved in LPS-induced inflammatory response of cardiomyocytes and NLRP3 inflammasome activation

As shown by qRT-PCR in Fig. 7, TLR4 mRNA expression levels in the LPS group increased significantly compared with control values (P<0.05); meanwhile, TLR4 mRNA amounts in the LPS+TAK-242 group were lower than those of the LPS group (P<0.05). TLR4 mRNA levels in the control+TAK-242 group were lower than control values, but with no significant difference (P>0.05).

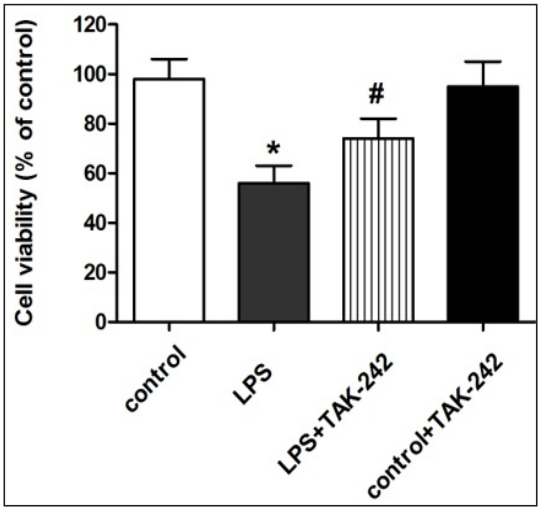

Fig. 6. Effects of TAK-242 on LPS-induced cell viability in cardiomyocytes. LPS, lipopolysaccharide. *P<0.05 vs. control group; #P<0.05 vs. LPS group.

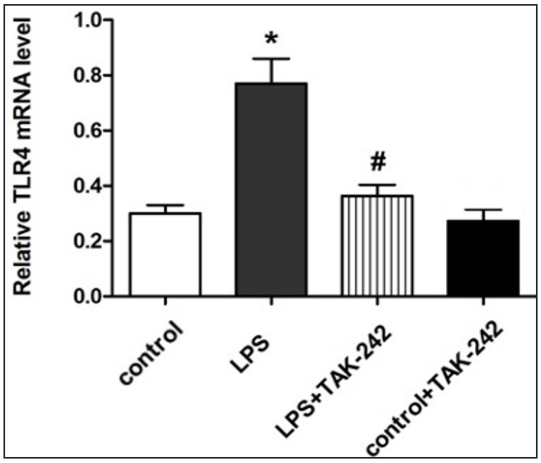

Fig. 7. TLR4 mRNA levels in cardiomyocytes as detected by fluorescence quantitative PCR. LPS, lipopolysaccharide. *P<0.05 vs. control group; #P<0.05 vs. LPS group.

Western blot data are summarized in Fig. 8. Compared with the control group, LPS treatment resulted in markedly increased expression levels of TLR4, MyD88, and NF-κB p65, as well as significant NLRP3 inflammasome activation, as reflected by significantly increased protein expression levels of NLRP3, ASC, and caspase-1 (P<0.05). Compared with the LPS group, the protein expression levels of TLR4, MyD88, and NF-κB p65 in the LPS+TAK-242 group were decreased significantly, while the NLRP3 inflammasome was inhibited, as reflected by significantly decreased NLRP3, ASC, and caspase-1 amounts (P<0.05). No significant differences were found in the protein expression levels of TLR4, MyD88, NF-κB p65, NLRP3, ASC, and caspase-1 between the control+TAK-242 and control groups (P>0.05).

ELISA data (Fig. 9) showed that TNF-α, IL-1β, and IL-18 expression levels were increased significantly in the LPS group compared with the control group (P<0.05). Meanwhile, TNF-α, IL-1β, and IL-18 amounts in the LPS+TAK-242 group were lower than those of the LPS group (P<0.05). There were no significant differences in the expression levels of TNF-α, IL-1β and IL-18 between the control+TAK-242 and control groups (P>0.05).

The above findings suggested that the TLR4/MyD88/NF-κB pathway participated in the inflammatory process of LPS-induced cardiomyocytes and promoted NLRP3 inflammasome activation.

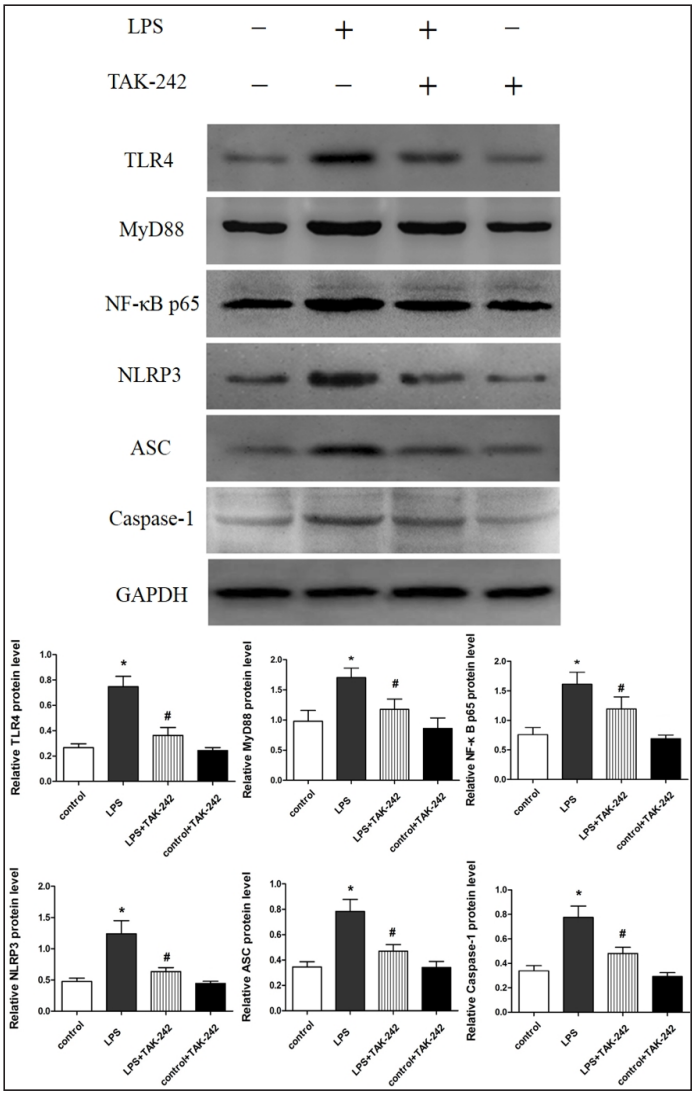

Fig. 8. TAK-242 inhibits LPS-induced TLR4 expression and NLRP3 inflammasome activation. LPS, lipopolysaccharide; NLRP3, Nod-like receptor protein 3. *P<0.05 vs. control group; #P<0.05 vs. LPS group.

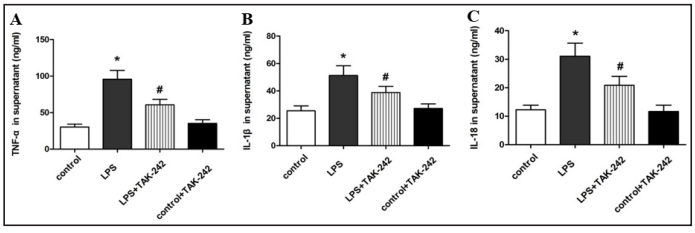

Fig. 9. Effects of TAK-242 on secreted TNF-α. (A), IL-1β (B), and IL-18 (C) in cultured cardiomyocytes. LPS, lipopolysaccharide. *P<0.05 vs. control group; #P<0.05 vs. LPS group.

Discussion

This study found that the inflammatory response in the myocardium after CME caused myocardial injury, with involvement of the TLR4/MyD88/NF-κB signaling pathway, which also activated the NLRP3 inflammasome, promoting the inflammatory cascade and aggravating myocardial injury. Blocking the TLR4/MyD88/NF-κB signaling pathway effectively improved CME-induced myocardial inflammation and reduced myocardial injury. In addition, *in vitro* assessment of cardiomyocytes further confirmed that TLR4/MyD88/NF-κB signaling played an important role in LPS-induced inflammation, which promoted NLRP3 inflammasome activation and aggravated inflammatory responses in cardiomyocytes. Inhibition of the TLR4/MyD88/NF-κB signaling pathway resulted in reduced LPS-induced inflammatory response in cardiomyocytes, inhibited NLRP3 inflammasome, and increased survival of cardiomyocytes.

CME is generally considered a spontaneous event in ischemic heart disease, or an iatrogenic complication of PCI [18]. The progressive loss of local systolic function in myocardial tissues during CME is not caused by myocardial microinfarction. Indeed, in myocardial tissues with complete loss of primary contractile function, micro-infarcts only account for 2% to 5% of perfusion area. Currently, it is believed that the inflammatory response in the myocardium might be the main cause of progressive systolic dysfunction [3, 19]. Our previous animal experiments demonstrated that large amounts of inflammatory cells infiltrate micro-infracted lesions in the myocardium after CME, accompanied with a massive release of inflammatory factors, leading to local inflammatory response in the myocardium; this could be considered the central cause of myocardial injury and progressive cardiac dysfunction after CME [20, 21]. Further experiments found that inflammatory factors in myocardial tissues, e.g. TNF-α and IL-1β, play important roles in CME-induced myocardial injury. After administration of related drugs (metoprolol and atorvastatin) to reduce inflammation, cardiac function was improved, with decreased myocardial injury [22, 23]. This study found increased levels of the myocardial enzyme in rats after CME, deteriorated cardiac function, micro-infracted lesions in myocardial tissues, and significantly increased serum levels of TNF-α, IL-1β, and IL-18, indicating that the model was successfully established, corroborating the pathophysiological changes of CME. Myocardial infarction leads to irreversible injury and necrosis of myocardial cells due to hypoxia and decreased adenosine triphosphate (ATP) supply. The necrotic cells activate their immune response after releasing their contents, resulting in acute inflammatory reaction, and excessive inflammatory reaction in turn causes myocardial injury [24]. In the CME dog model, Skyschally et al. found that the expression of TNF-α increased significantly in ischemic myocardial tissues, and they were mainly located in leukocyte infiltration foci and the periphery of micro-infarct foci. After glucocorticoid anti-inflammatory treatment, TNF-α expression was significantly down-regulated, which prevented progressive contractile dysfunction [25]. In the present study, micro-infarction was found to occur first that led to myocardial inflammation. However, inflammatory response also aggravated myocardial injury after myocardial infarction that led to the enlargement of myocardial infarct area. After the excessive inflammatory response in the myocardium was inhibited, myocardial injury was relieved and myocardial micro-infarct area decreased.

When the body is stimulated by external stimuli, innate immunity is first triggered, with induction of TLR4 expression, leading to adaptive immune responses; NF-κB is then activated through the MyD88-dependent signal transduction pathway. Some endogenous ligands activate NF-κB through the activation of TLR4 receptor, resulting in the release of pro-inflammatory factors such as TNF- a, IL-1β, and others [26]. The increased production and release of pro-inflammatory factors further activates NF-κB, which induces the NLRP3 inflammasome, leading to the continuous amplification of initial inflammatory signals, thus causing the so-called inflammatory waterfall effect [27, 28]. This study found that TLR4/MyD88/NF-κB signaling was significantly activated after CME, and participated in the inflammatory responses of the myocardium, resulting in decreased cardiac function and

myocardial injury in rats. The TLR4 specific inhibitor TAK-242 significantly inhibited TLR4/MyD88/NF-κB signaling, reduced NLRP3 inflammasome activation, and decreased the expression levels of TNF-α, IL-1β, IL-18, and other inflammatory factors; this resulted in significantly decreased CME-induced myocardial injury and improved cardiac function.

LPS, the main outer membrane component of Gram-negative bacteria, induces inflammatory responses in cardiomyocytes mainly via TLR4. When TLR4 binds to the corresponding ligand, it further activates NF-κB, promoting the upregulation of various inflammatory cytokines [29]. Therefore, to further clarify the role of TLR4/MyD88/NF-κB signaling in CME-induced myocarditis, an *in vitro* model of LPS-induced inflammation in neonatal rat cardiomyocytes was used in this study. The results showed that LPS treatment caused significantly activated TLR4/MyD88/NF-κB signaling pathway, activated NLRP3 inflammasome, increased expression levels of pro-inflammatory factors such as TNF-α, IL-1β, and IL-18, and markedly decreased survival of cardiomyocytes. After TAK-242 pre-treatment, the survival rate of LPS-induced cardiomyocytes was markedly increased. This effect was associated with reduced LPS-induced inflammatory response (decreased levels of TNF-α, IL-1β and IL-18) in cardiac cardiomyocytes, with subsequent reduction of NLRP3 inflammasome activation, by inhibiting the TLR4/MyD88/NF-κB signaling pathway.

The limitations of this study should be mentioned. Plastic microspheres were used as a micro-embolic agent in the current CME model. Although the model showed the physical properties of microvascular embolization, it did not display biological properties such as thrombus activity, vasoactivity, chemotaxis, and inflammation. In addition, clinical microvascular embolism is very complex, and involves platelets, leukocytes, and red cells, as well as atheromatous plaque components. Therefore, there is a certain gap with the actual pathophysiological changes of CME after plaque rupture.

In conclusion, this study demonstrated that the TLR4/MyD88/NF-κB signaling pathway participates in myocardial inflammation after CME and activates the NLRP3 inflammasome, promoting the inflammatory cascade and aggravating myocardial injury. Inhibition of this pathway effectively reduced CME-induced myocardial injury mainly by decreasing inflammatory responses in cardiomyocytes. Therefore, inhibiting TLR4/MyD88/NF-κB signaling may help reduce myocardial injury and improve cardiac function after CME. These findings provide novel insights into the prevention and treatment of CME-induced myocardial injury.

Acknowledgements

This study was supported by a grant from National Natural Science Foundation of China (Grant No. 81600283) and Guangxi Natural Science Foundation (Grant No. 2016GXNSFBA380022). “Medical Excellence Award”Funded by the Creative Research Development Grant from the First Affiliated Hospital of Guangxi Medical University

Disclosure Statement

This paper has not been published elsewhere in whole or in part. All authors have read and approved the content, and agree to submit for consideration for publication in the journal. There are no any ethical/legal conflicts involved in the article.

References

1 Heusch G, Skyschally A, Kleinbongard P: Coronary microembolization and microvascular dysfunction. Int J Cardiol 2018;pii:S0167-5273(17)37836-1.

2 Canton M, Skyschally A, Menabò R, Boengler K, Gres P, Schulz R, Haude M, Erbel R, Di Lisa F, Heusch G: Oxidative modification of tropomyosin and myocardial dysfunction following coronary microembolization. Europ Heart J 2006;27:875-881.
3 Dörge H, Neumann T, Behrends M, Skyschally A, Schulz R, Kasper C, Erbel R, Heusch G: Perfusion-contraction mismatch with coronary microvascular obstruction: role of inflammation. Am J Physiol Heart Circ Physiol 2000;279:H2587-H2592.
4 Li S, Zhong S, Zeng K, Luo Y, Zhang F, Sun X, Chen L: Blockade of NF-κB by pyrrolidinedithiocarbamate attenuates myocardial inflammatory response and ventricular dysfunction following coronary microembolization induced by homologous microthrombi in rats. Basic Res Cardiol 2010;105:139-150.
5 Li L, Zhao X, Lu Y, Huang W, Wen W: Altered expression of pro-and anti-inflammatory cytokines is associated with reduced cardiac function in rats following coronary microembolization. Mol Cell Biochem 2010;342:183-190.
6 Lundberg A M, Ketelhuth D F J, Johansson M E, Gerdes N, Liu S, Yamamoto M, Akira S, Hansson GK: Toll-like receptor 3 and 4 signaling through the TRIF and TRAM adaptors in haematopoietic cells promotes atherosclerosis. Cardiovasc Res 2013;99:364-373.
7 Chimenti C, Verardo R, Scopelliti F, Grande C, Petrosillo N, Piselli P, De Paulis R, Frustaci A: Myocardial expression of Toll-like receptor 4 predicts the response to immunosuppressive therapy in patients with virus-negative chronic inflammatory cardiomyopathy. Eur J Heart Fail 2017;19:915-925.
8 Lu M, Tang F, Zhang J, Luan A, Mei M, Xu C, Zhang S, Wang H, Maslov LN: Astragaloside IV Attenuates Injury Caused by Myocardial Ischemia/Reperfusion in Rats via Regulation of Toll-Like Receptor 4/Nuclear Factor-κB Signaling Pathway. Phytother Res 2015;29:599-606.
9 Soraya H, Clanachan A S, Rameshrad M, Maleki-Dizaji N, Ghazi-Khansari M, Garjani A: Chronic treatment with metformin suppresses toll-like receptor 4 signaling and attenuates left ventricular dysfunction following myocardial infarction. Eur J Pharmacol 2014;737:77-84.
10 Zhang J, Zhang J, Yu P, Chen M, Peng Q, Wang Z, Dong N: Remote Ischaemic Preconditioning and Sevoflurane Postconditioning Synergistically Protect Rats from Myocardial Injury Induced by Ischemia and Reperfusion Partly via Inhibition TLR4/MyD88/NF-κB Signaling Pathway. Cell Physiol Biochem 2017;41:22-32.
11 Ma S R, Xie X W: NLRC5 deficiency promotes myocardial damage induced by high fat diet in mice through activating TLR4/NF-κB. Biomed Pharmacother 2017;91: 755-766.
12 Wang Q, Lin P, Li P, Feng L, Ren Q, Xie X, Xu J: Ghrelin protects the heart against ischemia/reperfusion injury via inhibition of TLR4/NLRP3 inflammasomepathway. Life Sci 2017;186:50-58.
13 Wang X, Lu Y, Sun Y, He WK, Liang JB, Li L: TAK-242 Protects Against Apoptosis in Coronary Microembolization-Induced Myocardial Injury in Rats by Suppressing TLR4/NF-κB Signaling Pathway. Cell Physiol Biochem 2017;41:1675-1683.
14 Li L, Li D H, Qu N, Wen WM, Huang WQ: The role of ERK1/2 signaling pathway in coronary microembolization-induced rat myocardial inflammation and injury. Cardiology 2010;117:207-215.
15 Su Q, Li L, Zhao J, Sun Y, Yang H: Effects of nicorandil on PI3K/Akt signaling pathway and its anti-apoptotic mechanisms in coronary microembolization in rats. Oncotarget 2017;8:99347-99358.
16 Su Q, Li L, Zhou Y, Wang J, Liu Y, Ma G: Induction of myocardial PDCD4 in coronary microembolization-related cardiac dysfunction: evidence from a large-animal study. Cell Physiol Biochem 2014;34:533-542.
17 Wang H, Bei Y, Shen S, Huang P, Shi J, Zhang J, Sun Q, Chen Y, Yang Y, Xu T, Kong X, Xiao J: miR-21-3p controls sepsis-associated cardiac dysfunction via regulating SORBS2. J Mol Cell Cardiol 2016;94:43-53.
18 Heusch G: The coronary circulation as a target of cardioprotection. Circ Res 2016;118:1643-1658.
19 Dörge H, Schulz R, Belosjorow S, Post H, van de Sand A, Konietzka I, Frede S, Hartung T, Vinten-Johansen J, Youker KA, Entman ML, Erbel R, Heusch G: Coronary microembolization: the role of TNF-α in contractile dysfunction. J Mol Cell Cardiol 2002;34:51-62.
20 Li L, Qu N, Li D H, Wen WM, Huang WQ: Coronary microembolization induced myocardial contractile dysfunction and tumor necrosis factor-α mRNA expression partly inhibited by SB203580 through a p38 mitogen-activated protein kinase pathway. Chin Med J (Engl) 2011;124:100-105.
21 Su Q, Li L, Zhao J, Sun Y, Yang H: MiRNA Expression Profile of the Myocardial Tissue of Pigs with Coronary Microembolization. Cell Physiol Biochem 2017;43:1012-1024.
22 Lu Y, Li L, Zhao X, Huang W, Wen W: Beta blocker metoprolol protects against contractile dysfunction in rats after coronary microembolization by regulating expression of myocardial inflammatory cytokines. Life Sci 2011;88:1009-1015.

23 Su Q, Li L, Liu T, Wang J, Zhou Y, Liu Y: Effects of atorvastatin on PDCD4/NF-κB/TNF-α signaling pathway during coronary microembolization of miniature pigs. Exp Mol Pathol 2015;99:564-569.
24 Oyamada S, Bianchi C, Takai S, Chu LM, Sellke FW: Chymase inhibition reduces infarction and matrix metalloproteinase-9 activation and attenuates inflammation and fibrosis after acute myocardial ischemia/reperfusion. J Pharmacol Exp Ther 2011;339:143-151.
25 Skyschally A, Haude M, Dörge H, Thielmann M, Duschin A, van de Sand A, Konietzka I, Büchert A, Aker S, Massoudy P, Schulz R, Erbel R, Heusch G: Glucocorticoid treatment prevents progressive myocardial dysfunction resulting from experimental coronary microembolization. Circulation 2004;109:2337-2342.
26 O'Neill L A J, Bowie A G: The family of five: TIR-domain-containing adaptors in Toll-like receptor signaling. Nat Rev Immunol 2007;7:353-364.
27 Zhang X, Du Q, Yang Y, Wang J, Dou S, Liu C, Duan J: The protective effect of Luteolin on myocardial ischemia/reperfusion (I/R) injury through TLR4/NF-κB/NLRP3 inflammasomepathway. Biomed Pharmacother 2017;91:1042-1052.
28 Huang Z, Zhuang X, Xie C, Hu X, Dong X, Guo Y, Li S, Liao X. Exogenous Hydrogen Sulfide Attenuates High Glucose-Induced Cardiotoxicity by Inhibiting NLRP3 Inflammasome Activation by Suppressing TLR4/NF-κB Pathway in H9c2 Cells. Cell Physiol Biochem 2016;40:578-1590.
29 Wang J, Zhang Y, Guo LL, Wu GJ, Liu RH: Salvianolic acid B inhibits the TLR4-NFκB-TNFα pathway and attenuates neonatal rat cardiomyocyte injury induced by lipopolysaccharide. Chin J Integr Med 2011;17:775-779.